Augmented excitation cross-section of gadolinium ions in nanostructured glasses

ROBERTO LORENZI[1*], ALBERTO PALEARI[1], VLADIMIR N. SIGAEV[2], ELENA S. IGNAT'EVA[2], NIKITA V. GOLUBEV[2]

[1]*Department of Materials Science, University of Milano-Bicocca, via Cozzi 55, 20125 Milano, Italy*
[2]*P.D. Sarkisov International Laboratory of Glass-based Functional Materials, Mendeleev University of Chemical Technology of Russia, Miusskaya Square 9, 125047 Moscow, Russia*
**Corresponding author: roberto.lorenzi@mater.unimib.it*

Received XX Month XXXX; revised XX Month, XXXX; accepted XX Month XXXX; posted XX Month XXXX (Doc. ID XXXXX); published XX Month XXXX

In this Letter, we present detailed absorption and emission data on nanostructured germanosilicate glasses and glassceramics containing Ga_2O_3 nanophases and doped with Gd ions. The results show that these systems are suitable hosts for the enhancement of excitation cross-section of rare earth ions *via* energy transfer from gallium oxide nanophase with a related quantum yield of 21%. The role of matrix composition and nanostructures morphology on the Gd emission is discussed. © 2015 Optical Society of America

OCIS codes: *(160.2540) Fluorescent and luminescent materials, (160.2750) Glass and other amorphous materials, (160.4236) Nanomaterials, (260.2160) Energy transfer, (260.2510) Fluorescence, (300.6280) Spectroscopy, fluorescence and luminescence*

http://dx.doi.org/10.1364/OL.99.099999

Rare earth (RE) ions represent one of the most important building blocks in the design of optical and photonic materials. Nevertheless, their optical activity can be fully exploited in practical applications only by incorporation in suitable host. In the last two decades, the choice of oxide nanoparticles as appropriate host has been thoroughly investigated for the fabrication of nanophosphors with possible application in display technology, lighting, sensing, bioimaging, and photonics [1-7]. In many cases, nanoparticles act not only as structural units for RE ion accommodation, but they also bring important functionalities. As a matter of fact, RE ions show high luminescence efficiency, but an efficient excitation is often prevented because of their low absorption cross sections. In this regard, oxide hosts can harvest the excitation energy and transfer it to the ion so as to increase the effective absorption cross section of the light emitting system and its luminescence efficiency. However, in many cases the implementation of real device based on free-standing nanoparticles is quite difficult as a result of agglomeration and degradation. For this reason many strategies have been studied for the incorporation of RE-doped nanoparticles in suitable matrix such as plastic and glasses [8-10]. The aim of these approaches is to obtain nanocomposites materials merging the optical functionality of RE-doped nanoparticles and the workability and inertness of the matrix, possibly in a fully transparent optical material. Here we present a new method for the incorporation of gadolinium ions in glasses and glassceramics containing gallium oxide nanostructures embedded in an amorphous germanosilicate matrix. The resulting material is fully transparent over the entire visible spectra, and effective energy transfer processes between oxide nanophase and RE ions have been quantified by time-resolved photoluminescence excitation (TRPLE) spectra. Samples of Gd-doped glass were prepared by the conventional melt-quenching method and using Li_2CO_3 (chemically pure), Na_2CO_3 (chemically pure), Ga_2O_3 (chemically pure), GeO_2 (special purity grade), SiO_2 (special purity grade), and Gd_2O_3 (special purity grade) as raw materials. The powders were weighed with an analytical balance so as to obtain batches of 40 g and accurately mixed in a mortar for at least 15 minutes. The mixture was then transferred in an 45 ml platinum crucible and melted in an electrically heated furnace at 1480 °C for 40 min. The melt was poured on stainless steel plate and quenched with another plate. Finally, the samples were cut and polished obtaining samples with dimension 1x1 cm^2 and 1 mm thick. Materials with different composition, summarized in Tab. 1, have been prepared with the purpose of studying the effect of gallium oxide concentration and matrix viscosity on the Gd emission features. Part of the samples was heat treated at exothermic peak extremum temperatures in DSC curves (not shown) reported in Tab. 1.

Table 1. Label, composition and thermal treatment of investigated samples

	Composition (mol%) + 0.1 Gd_2O_3					Thermal
Sample	Ga_2O_3	SiO_2	GeO_2	Li_2O	Na_2O	treatment
25/23G	25.0	23.5	42.2	7.0	2.3	As quenched
25/23GC	25.0	23.5	42.2	7.0	2.3	676°C, 15 min
20/35G	20.0	35.0	35.0	7.5	2.5	As quenched
20/35GC	20.0	35.0	35.0	7.5	2.5	694°C, 15 min
20/25G	20.0	25.0	45.0	7.5	2.5	As quenched
20/25GC	20.0	25.0	45.0	7.5	2.5	684°C, 15 min

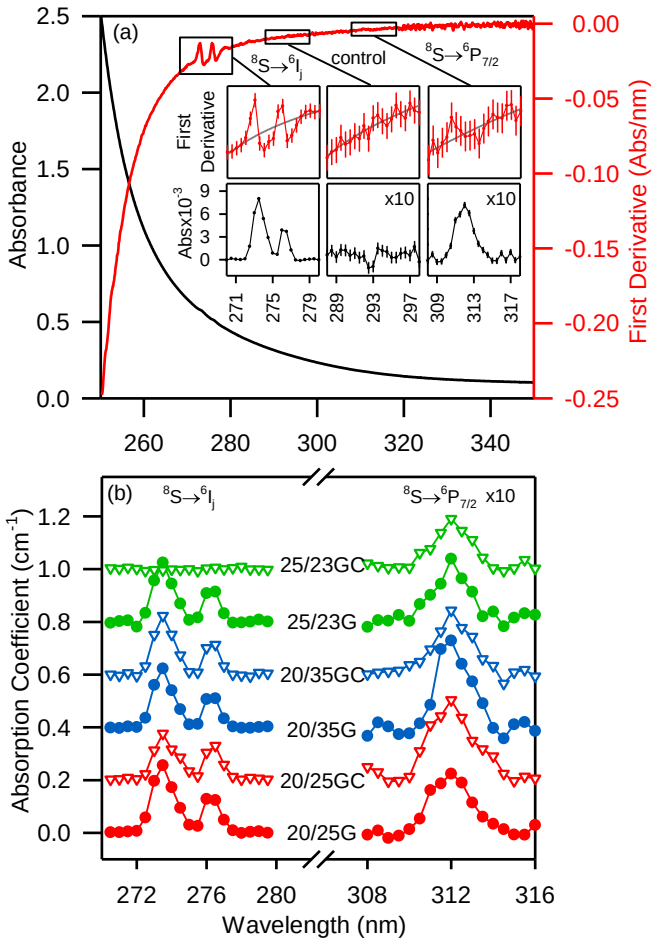

Fig. 1. Analysis of absorption spectra: (a) UV absorption spectrum of sample 20/25G (black line, left axis) and 1st derivative (red line, right axis). In the inset: magnified 1st derivative (upper panel) in the region of Gd absorption lines and, as comparison, in a control region without signal. Data points have been quantified by running average, error bars represent standard deviation of data in noisy spectral region, and grey lines are baseline curves calculated as 4th order polynomials. Integrated 1st derivative after baseline correction (lower panel). (b) Results of absorption spectra analysis. Spectra in the region of $^8S_{7/2}\rightarrow{}^6P_{7/2}$ transition are multiplied by a factor 10, spectra are upshifted for clarity. Transition $^8S_{7/2}\rightarrow{}^6I_j$ for sample 25/23GC is undetectable because of the huge absorption in this sample by nanophase band-to-band transitions.

This treatment leads to the formation of glassceramics since it induces partial crystallization of the matrix, *via* atom diffusion, with the formation of γ-Ga_2O_3 nanocrystals (NCs) with dimensions of 6±2 nm in diameter and with a concentration of 10^{17}-10^{18} NC/cm^3 [11]. It is worth to note that the presence of 0.1 mol% of Gd ions does not alter the overall nanomorphology of glasses and glassceramics. The x-ray diffraction patterns and TEM analysis (not shown) confirm both the presence of gallium oxide nanoheterogeneities and nanocrystals in glasses and glassceramics, respectively, as previously reported [12]. The optical transmission of these samples is very high in the visible range (about 80%), thanks to the low refractive index mismatch between nanostructures and matrix and the very low dimensions of the precipitated phase, with an optical absorption edge ranging between 4.5 and 4.6 eV depending on composition and thermal treatment [11]. A representative example of UV absorption spectra for sample 20/25G is reported in Fig. 1a. Gd doping leads to minor

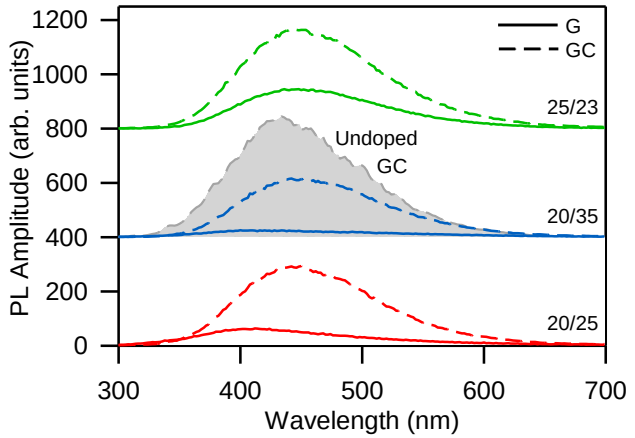

Fig. 2. DAP recombination PL emission spectra excited at 250 nm of Gd-doped glass and glassceramic samples. For comparison, spectrum of undoped glassceramic sample with molar composition 20Ga_2O_3-35SiO_2-35GeO_2-7.5Li_2O-2.5Na_2O (filled grey line) is reported. Spectra are upshifted for clarity.

absorption features that can be evidenced by plotting the 1st derivative of absorption spectrum. Specific signals ascribable to RE ions can be detected: a doublet in the region 271-279 nm and a single peak in the region 309-317 nm which correspond to the $^8S_{7/2}\rightarrow{}^6I_j$ and $^8S_{7/2}\rightarrow{}^6P_{7/2}$ transitions, respectively. In order to determine the oscillator strengths of the involved transitions, absorption spectrum has been re-constructed by numerical integration of the baseline-corrected 1st derivative spectrum in the regions of interest. The results are summarized in Fig. 1b and Tab. 2. The analysis confirms the strong forbidden nature of the *f-f* transitions with oscillator strengths with values ranging from $1.5\cdot10^{-7}$ to $2.0\cdot10^{-7}$ and from $1.4\cdot10^{-6}$ to $2.4\cdot10^{-6}$ for $^8S_{7/2}\rightarrow{}^6P_{7/2}$ and $^8S_{7/2}\rightarrow{}^6I_j$ transition, respectively, consistent with values of gadolinium incorporated in other glassy systems [13, 14]. Remarkably, shape, position, and strength of these absorption lines scarcely depend on composition and thermal treatments, suggesting that nature, location and number of Gd nearest neighbors is fixed and does not change with glass composition or upon nanostructuring. Even though, on the one hand, the addition of Gd ions does not alter significantly morphology and absorption features of glass and glassceramics, on the other hand, it strongly alters the optical emission features of these samples. In fact, NCs enable for strong blue emission centered at about 460 nm and excited by band-to-band transitions and related to radiative recombination of donor-acceptor pairs (DAP) due to defect states [11, 15]. As reported in Fig. 2, the intensity of this emission, excited at 250 nm, is always enhanced by thermal treatments, since DAP formation is promoted by the crystallization of nanoheterogeneities in NCs. Interestingly, its amplitude is partially suppressed by the presence of Gd ions. Specifically the intensity of blue luminescence in sample 20/35GC is about two times higher for undoped sample with respect to Gd containing glassceramic. This outcome gives us a first hint about the occurrence of energy transfer (ET) processes, in which the Gd ions act as acceptor species that partially collect energy transferred from NCs DAP recombination acting as donor species. To further investigate this aspect, we have collected excitation and emission patterns of Gd-related emission, the results are summarized in Fig. 3. Photoluminescence (PL) spectra were collected exciting at 276 nm corresponding to the $^8S_{7/2}\rightarrow{}^6I_j$ transition of Gd ions. The resulting PL shows two main peaks: a sharp peak located at 313 nm originated by intra-center relaxation of Gd ions $^6P_j\rightarrow{}^8S_{7/2}$ and the already discussed broad band located at 450 nm from DAP recombination. Interestingly, the photoluminescence excitation (PLE) spectrum of the $^6P_j\rightarrow{}^8S_{7/2}$ line, gray colors in Fig. 3a, includes not only

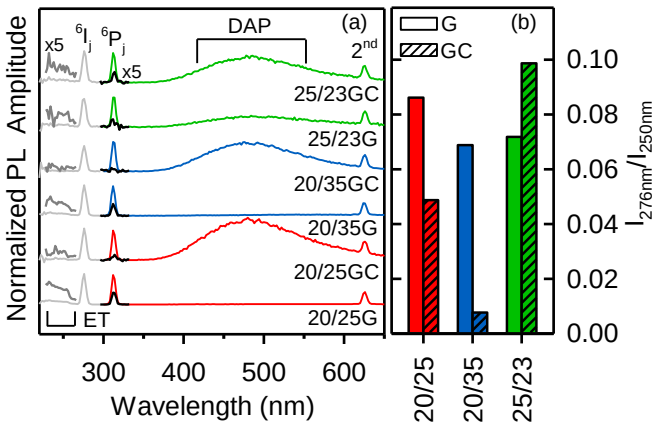

Fig. 3. (a) Gd-related PL (colored lines: excitation wavelength at 276 nm, black lines in correspondence of ^6P_j emission refer to energy-transfer mediated excitation at 250 nm and are multiplied by a factor x5) and PLE (grey lines, emission wavelength at 313 nm, dark grey lines are multiplied by a factor x5) spectra of glass and glassceramic samples. Spectra have been collected with a time delay of 50 ms between lamp flash and signal acquisition. Spectra are upshifted for clarity. (b) Amplitude ratio of excitation efficiency of direct intra-center Gd excitation (PL amplitude at 313 nm when excited at 276 nm) and from Ga_2O_3 energy transfer excitation (PL amplitude at 313 nm when excited at 250 nm) of ^6P_j Gd emission line.

the sharp peak at 276 nm, but also a broad band spanning from 220 nm up to 260 nm. The origin of this band cannot be attributed to Gd ions and, instead, it is consistent with an ET process. The Ga-oxide, either in form of nanoheterogeneity or nanocrystals, can harvest a much broader part of UV spectrum and subsequently transfer this energy to Gd ions. The result is an increase of the effective absorption cross-section of Gd ions excitation. However, the intensity of this effect is strongly sample-dependent. For this reason, we have calculated, as possible figure of merit, the ratio between the light emitted at 313 nm when excited *via* intra-center configuration (i.e. excitation at 276 nm) and *via* ET from Ga-oxide phase (i.e. excitation at 250 nm). The results of this comparison are reported in Fig. 3b. The higher efficiency of about 10% is observed for sample 25/23GC for which the molar content of Ga_2O_3 NCs is the highest. Unexpectedly, high values of this parameter are registered also for glass samples, indicating that the ET can occur already in presence of nanoheterogeneities of Ga-oxide before the formation of nanocrystalline domains. In fact, DAP recombination is observed even for glass samples where the presence of Ga-enriched oxide phases involves the formation of the defects responsible for the blue emission, as we can see in the non-negligible 460 nm luminescence reported in Figs. 2 and 3a. For samples 20/25 and 20/35 the efficiency is even reduced after thermal treatment (see Fig. 3b), possibly because Gd ions tend to be allocated outside the NC phase, whereas the number of DAP inside NCs increases, with a resulting increase of mean donor-acceptor distance and a lower ET efficiency. The higher content of Ga in sample 25/35 is enough to compensate such an effect and ensuring a closer distance between NCs and Gd ions, hence showing a higher ET efficiency. Moreover, from data reported in Fig. 3b some conclusions about the role of Ge content in the melt composition can be drawn. Germanium ions modify glass networking and it is known that the melt viscosity of germanosilicate matrix is lowered by the presence of this metal [16]. Even the nanostructuring processes are strongly affected by the presence of germanium in the glass matrix. In fact, it is known that the presence of Ga_2O_3 nanophases in the glass, as well as the crystallization of γ-Ga_2O_3, are preferentially formed in GeO_2-enriched zones [17]. Accordingly,

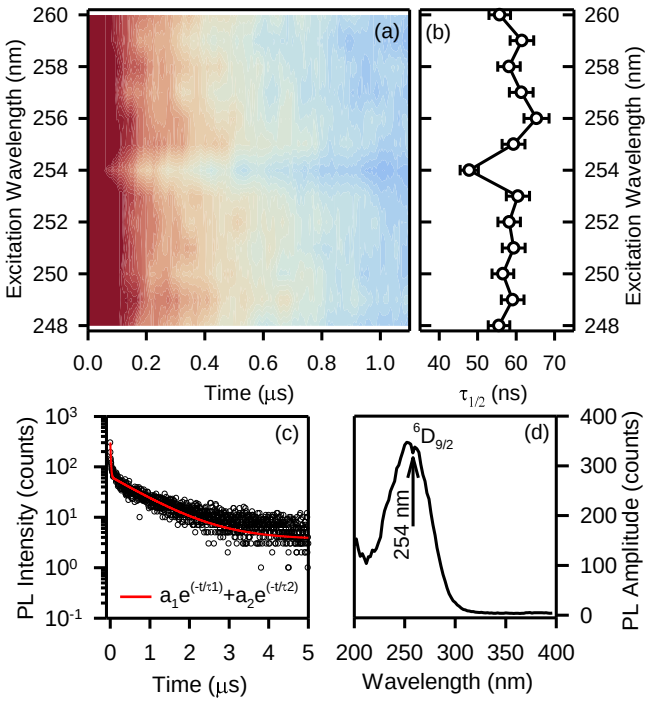

Fig. 4. (a) TRPLE map of DAP recombination, with emission wavelength fixed at 460 nm. (b) Half-life decay time as a function of excitation wavelength, data reported in (a) have been fitted with a double exponential function. (c) Example of decay fitting measured in correspondence of the valley visible in (a) and (b) at an excitation wavelength of 254 nm and emission wavelength at 460 nm. (d) PLE spectra of DAP recombination showing a deep at 254 nm corresponding to the $^8S_{7/2}\rightarrow{}^6D_{9/2}$ absorption line of Gd ions. All data have been collected on sample 25/23GC.

sample 25/23 presents two advantages on ET processes with respect to other compositions: 1) a higher content of Ga, which favors a closer distance between NCs and Gd ions, and 2) a high content of Ge, which promotes the formation of Ga-enriched nanophases within the matrix. We highlight that the outcomes discussed till now are only an indication of ET process, i.e. the presence of an additional excitation channel for Gd emission is a condition necessary, but not sufficient, for establishing the occurrence of ET. The nature of the process can be more accurately assessed by the dynamic features of the involved transitions. For this reason, we have conducted TRPLE experiment to deeply characterize sample 25/23GC. The contour plot of TRPLE is reported in Fig. 4a. We monitored the decay time of the donor species - decay time registered at 460 nm, with a band pass of 2.5 nm - as a function of excitation wavelength. At 254 nm there is a valley, that clearly indicates a decay shortening of DAP recombination when excited at this wavelength, in correspondence of energy transfer to the ^6D_j line of Gd^{3+}. Energy transfer quantum yield (QY_{ET}) can be calculated by comparing the decay times of the donor species when excited in correspondence of the ^6D_j absorption line of the acceptor (τ_{DA}) and in the region of band-to-band excitation (τ_B): $QY_{ET} = 1 - \tau_{DA}/\tau_B$ [18]. In fact, the presence of a further de-excitation channel, due to energy transfer, increases the probability of non-radiative paths of the excited donor species resulting in a shortening of the radiative lifetime. This shortening is evident in Fig. 4b where the half-life time of the donor is plotted as a function of excitation wavelength and a drop of ~15 ns is observed at 254 nm. Indeed, the kinetic of DAP recombination is not a pure single exponential and can be fitted by a double exponential function, as shown in Fig. 4c. As a consequence, we adopted the half-life

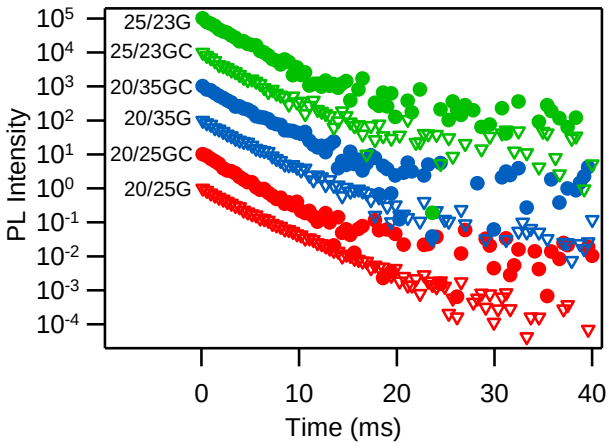

Fig. 5. PL decay curves of $^6P_J \rightarrow {}^8S_{7/2}$ transition in glass and glassceramic doped with 0.1%mol of Gd_2O_3, with excitation and emission wavelengths fixed at 276 and 313 nm, respectively.

decay time as reliable indicator of the overall lifetime. Accordingly, the calculated values of τ_{DA} (at 254 nm) and τ_B (at 253 nm) are 47.8 and 60.5 ns, respectively, and the resulting QY_{ET} is 21±5 %. Experimental evidences of ET process are also confirmed by the presence of a deep at 254 nm in the excitation spectra of DAP recombination, as reported in Fig. 4d. Finally, to prove that our approach is a convenient method for Gd incorporation in glassy-like materials, we have measured lifetime of intra-center $^6P_J \rightarrow {}^8S_{7/2}$ emission so as to evaluate emission QY from Strickler-Berg analysis [19]. The results are summarized in Fig. 5, where the decay profiles of our samples are reported with excitation wavelength at 276 nm and emission wavelength at 313 nm. Interestingly, the decay times measured for our samples is of 2.8 msec with a statistical dispersion in the measured sample set, calculated as standard deviation, of 7%. This outcome reveals that the local environment of Gd^{3+} ions is not critically modified by glass composition and especially by nanocrystal formation, thus evidencing the propensity of Gd ions to be dispersed outside the crystalline nanophase with a preferential location in the amorphous matrix. This view is also supported by the high difference between the effective ionic radius of Ga^{3+} (62 pm) and Gd^{3+} (94 pm) ions in oxides that prevents a favorable condition for atomic substitution of cationic sites in the γ-Ga_2O_3 nanophase [20]. Finally, from Strickler-Berg analysis carried out on absorption and emission spectra we have evaluated the expected maximum lifetime τ_0 of Gd transition in absence of any competitive decay channel [21]:

$$1/\tau_0 = 2.88 \cdot 10^{-9} n^2 \frac{\int F(\nu) d\nu}{\int \nu^{-3} F(\nu) d\nu} \int \frac{\varepsilon(\nu)}{\nu} d\nu \qquad \textbf{(1)}$$

Where n≈1.6 is the refractive index [17], F is the emission spectra expressed in arbitrary units vs. wavenumber, and $\varepsilon=\alpha/(\ln(10)\cdot c)$ is the molar extinction coefficient vs. wavenumber, related to the absportion coefficient α in cm^{-1} and the molar concentration c in mol_{Gd}/L_{glass}. The calculated lifetime has then been compared with the effective lifetimes τ reported in Fig. 5 and Tab. 2 to calculate the emission quantum yield $QY = \tau/\tau_0$. The results, summarized in Tab. 2, show that the value is close to unity within the experimental error for all the investigated samples demonstrating that the proposed host glass and glassceramics are suitable hosts for the incorporation of Gd ions. In conclusion, we have presented a new approach to the enhancement of effective absorption cross-section of Gd ions in germanosilicate matrix, by means of Ga oxide nanostructures. The detailed optical analysis evidences the occurrence of energy transfer processes between DAP recombination and RE ions. Furthermore, the analysis highlights the role of glass composition and nanostructuring in governing these energy transfer processes. Based on our experimental evidences and the high discrepancy between Gd and Ga ionic radius, the preferential location of the dopant ions have been assessed to be in the amorphous matrix even after nanocrystal formation in glassceramic samples. However, the emission quantum yield of Gd ions has been quantified to be of order unity confirming that our approach is suitable as RE host without degradation of the overall efficiency of Gd intrinsic emission.

Table 2. Oscillator strengths, Gd molarity, lifetimes calculated according to Eq. 1, measured lifetimes, and calculated Quantum Yield of $^6P_J \rightarrow {}^8S_{7/2}$ transition. Experimental error on QY is ±25%.

	f (·10⁸)					
Sample	$^6P_{7/2}$	^6I_j	C_{Gd} (mM)	τ_0 (ms)	τ (ms)	QY (%)
25/23G	15.8	218	64.4	3.64	2.53	70
25/23GC	15.7	n.d.	57.1	3.65	2.62	72
20/35G	20.5	156	74.8	2.79	2.87	103
20/35GC	17.2	173	70.8	3.33	2.99	90
20/25G	19.8	242	60.0	2.9	2.58	89
20/25GC	20.0	144	73.5	2.87	3.02	105

Funding. Cariplo Foundation (2012-920), Ministry of Education and Science of the Russian Federation (14.Z50.31.0009 and MK 8807.2016.3).

References

1. M. Back, E. Trave, R. Marin, N. Mazzucco, D. Cristofori, and P. Riello, J. Phys. Chem. C **118**, 30071 (2014).
2. T. Zako, M. Yoshimoto, H. Hyodo, H. Kishimoto, M. Ito, K. Kaneko, K. Soga, and M. Maeda, Biomater. Sci. **3**, 59 (2015).
3. R. Lorenzi, A. Paleari, N. V. Golubev, E. S. Ignat'eva, V. N. Sigaev, M. Niederberger, and A. Lauria, J. Mat. Chem. C **3**, 41 (2015).
4. J. Reszczyńska, T. Grzyb, J. W. Sobczak, W. Lisowski, M. Gazda, B. Ohtani, and A. Zaleska, Appl. Catal. B-Environ. **163**, 40 (2015).
5. S. Hao, G. Chen, and C. Yang, Theranostics **3**, 331 (2013).
6. M. Alkahtani, Y. Chen, J. J. Pedraza, J. M. González, D. Y. Parkinson, P. R. Hemmer, and H. Liang, Opt. Express **25**, 1030 (2017).
7. X. Jin, H. Li, D. Li, Q. Zhang, F. Li, W. Sun, Z. Chen, and Q. Li, Opt. Express **24**, A1276 (2016).
8. N. Wan, J. Xu, T. Lin, X. Zhang, and L. Xu, Appl. Phys. Lett. **92**, 201109 (2008).
9. N. Dantas, E. Serqueira, A. Carmo, M. Bell, V. Anjos, and G. Marques, Opt. Lett. **35**, 1329 (2010).
10. S. Brovelli, N. Chiodini, F. Meinardi, A. Monguzzi, A. Lauria, R. Lorenzi, B. Vodopivec, M. Mozzati, and A. Paleari, Phys. Rev. B **79**, 153108 (2009).
11. V. N. Sigaev, N. V. Golubev, E. S. Ignat'eva, A. Paleari, and R. Lorenzi, Nanoscale **6**, 1763 (2014).
12. V. N. Sigaev, N. V. Golubev, E. S. Ignat'eva, B. Champagnon, D. Vouagner, E. Nardou, R. Lorenzi, and A. Paleari, Nanoscale **5**, 299 (2013).
13. R. Reisfeld, E. Greenberg, R. Velapoldi, and B. Barnett, J. Chem. Phys. **56**, 1698 (1972).
14. J. Kliava, I. Edelman, A. Potseluyko, E. Petrakovskaja, R. Berger, I. Bruckental, Y. Yeshurun, A. Malakhovskii, and T. Zarubina, J. Phys.: Condens. Matter **15**, 6671 (2003).
15. A. Paleari, N. V. Golubev, E. S. Ignat'eva, V. N. Sigaev, A. Monguzzi, and R. Lorenzi, ChemPhysChem (2017).
16. D. Sanditov, J. Exp. Theor. Phys. **110**, 675 (2010).
17. A. Paleari, V. Sigaev, N. Golubev, E. Ignat'eva, S. Bracco, A. Comotti, A. Azarbod, and R. Lorenzi, Acta Mater. **70**, 19 (2014).
18. J. R. Lakowicz, "Energy transfer," in *Principles of fluorescence spectroscopy* (Springer, 1999), pp. 367.
19. S. Strickler and R. A. Berg, J. Chem. Phys. **37**, 814 (1962).
20. R. Shannon and C. T. Prewitt, Acta Crystallogr. B **25**, 925 (1969).
21. W. W. Parson, *Modern optical spectroscopy* (Springer, 2007).

Plain References

1. M. Back, E. Trave, R. Marin, N. Mazzucco, D. Cristofori, and P. Riello, "Energy Transfer in Bi-and Er-Codoped Y2O3 Nanocrystals: An Effective System for Rare Earth Fluorescence Enhancement," J. Phys. Chem. C 118, 30071-30078 (2014).
2. T. Zako, M. Yoshimoto, H. Hyodo, H. Kishimoto, M. Ito, K. Kaneko, K. Soga, and M. Maeda, "Cancer-targeted near infrared imaging using rare earth ion-doped ceramic nanoparticles," Biomater. Sci. 3, 59-64 (2015).
3. R. Lorenzi, A. Paleari, N. V. Golubev, E. S. Ignat'eva, V. N. Sigaev, M. Niederberger, and A. Lauria, "Non-aqueous sol–gel synthesis of hybrid rare-earth-doped γ-Ga 2 O 3 nanoparticles with multiple organic–inorganic-ionic light-emission features," J. Mat. Chem. C 3, 41-45 (2015).
4. J. Reszczyńska, T. Grzyb, J. W. Sobczak, W. Lisowski, M. Gazda, B. Ohtani, and A. Zaleska, "Visible light activity of rare earth metal doped (Er 3+, Yb 3+ or Er 3+/Yb 3+) titania photocatalysts," Appl. Catal. B-Environ. 163, 40-49 (2015).
5. S. Hao, G. Chen, and C. Yang, "Sensing using rare-earth-doped upconversion nanoparticles," Theranostics 3, 331-345 (2013).
6. M. Alkahtani, Y. Chen, J. J. Pedraza, J. M. González, D. Y. Parkinson, P. R. Hemmer, and H. Liang, "High resolution fluorescence bio-imaging upconversion nanoparticles in insects," Opt. Express 25, 1030-1039 (2017).
7. X. Jin, H. Li, D. Li, Q. Zhang, F. Li, W. Sun, Z. Chen, and Q. Li, "Role of ytterbium-erbium co-doped gadolinium molybdate (Gd 2 (MoO 4) 3: Yb/Er) nanophosphors in solar cells," Opt. Express 24, A1276-A1287 (2016).
8. N. Wan, J. Xu, T. Lin, X. Zhang, and L. Xu, "Energy transfer and enhanced luminescence in metal oxide nanoparticle and rare earth codoped silica," Appl. Phys. Lett. 92, 201109 (2008).
9. N. Dantas, E. Serqueira, A. Carmo, M. Bell, V. Anjos, and G. Marques, "Energy transfer between CdS nanocrystals and neodymium ions embedded in vitreous substrates," Opt. Lett. 35, 1329-1331 (2010).
10. S. Brovelli, N. Chiodini, F. Meinardi, A. Monguzzi, A. Lauria, R. Lorenzi, B. Vodopivec, M. Mozzati, and A. Paleari, "Confined diffusion of erbium excitations in SnO 2 nanoparticles embedded in silica: a time-resolved infrared luminescence study," Phys. Rev. B 79, 153108 (2009).
11. V. N. Sigaev, N. V. Golubev, E. S. Ignat'eva, A. Paleari, and R. Lorenzi, "Light-emitting Ga-oxide nanocrystals in glass: a new paradigm for low-cost and robust UV-to-visible solar-blind converters and UV emitters," Nanoscale 6, 1763-1774 (2014).
12. V. N. Sigaev, N. V. Golubev, E. S. Ignat'eva, B. Champagnon, D. Vouagner, E. Nardou, R. Lorenzi, and A. Paleari, "Native amorphous nanoheterogeneity in gallium germanosilicates as a tool for driving Ga 2 O 3 nanocrystal formation in glass for optical devices," Nanoscale 5, 299-306 (2013).
13. R. Reisfeld, E. Greenberg, R. Velapoldi, and B. Barnett, "Luminescence quantum efficiency of Gd and Tb in borate glasses and the mechanism of energy transfer between them," J. Chem. Phys. 56, 1698-1705 (1972).
14. J. Kliava, I. Edelman, A. Potseluyko, E. Petrakovskaja, R. Berger, I. Bruckental, Y. Yeshurun, A. Malakhovskii, and T. Zarubina, "Magnetic and optical properties and electron paramagnetic resonance of gadolinium-containing oxide glasses," J. Phys.: Condens. Matter 15, 6671 (2003).
15. A. Paleari, N. V. Golubev, E. S. Ignat'eva, V. N. Sigaev, A. Monguzzi, and R. Lorenzi, "Donor-acceptor control in grown-in-glass Ga-oxide nanocrystals by crystallization-driven heterovalent doping," ChemPhysChem (2017).
16. D. Sanditov, "Shear viscosity of glass-forming melts in the liquid-glass transition region," J. Exp. Theor. Phys. 110, 675-688 (2010).
17. A. Paleari, V. Sigaev, N. Golubev, E. Ignat'eva, S. Bracco, A. Comotti, A. Azarbod, and R. Lorenzi, "Crystallization of nanoheterogeneities in Ga-containing germanosilicate glass: Dielectric and refractive response changes," Acta Mater. 70, 19-29 (2014).
18. J. R. Lakowicz, "Energy transfer," in Principles of fluorescence spectroscopy (Springer, 1999), pp. 367-394.
19. S. Strickler and R. A. Berg, "Relationship between absorption intensity and fluorescence lifetime of molecules," J. Chem. Phys. 37, 814-822 (1962).
20. R. Shannon and C. T. Prewitt, "Effective ionic radii in oxides and fluorides," Acta Crystallogr. B 25, 925-946 (1969).
21. W. W. Parson, Modern optical spectroscopy (Springer, 2007)